

1 **Efficient system reliability analysis for layered soil slopes with multiple**
2 **failure modes using sequential compounding method**

3 Kang Liao¹, Yiping Wu^{2, *}, Fasheng Miao³, Longfei Zhang⁴, Michael Beer⁵

4 ¹ Assistant Professor, Faculty of Geosciences and Environmental Engineering, Southwest Jiaotong
5 University, Chengdu 610031, China. Email: liaokang@swjtu.edu.cn

6 ² Professor, Faculty of Engineering, China University of Geosciences, Wuhan 430074, China. Email:
7 ypwu@cug.edu.cn

8 ³ Associate Professor, Faculty of Engineering, China University of Geosciences, Wuhan 430074,
9 China. Email: fsmiao@cug.edu.cn

10 ⁴ Ph.D. Candidate, Faculty of Engineering, China University of Geosciences, Wuhan 430074, China.
11 Email: longfeizhang@cug.edu.cn

12 ⁵ Professor, Institute for Risk and Reliability, Leibniz University Hannover, Hanover 30167,
13 Germany. Email: beer@irz.uni-hannover.de

14

15 **Abstract**

16 Evaluating the system reliability of layered soil slopes is a challenging issue because multiple failure
17 modes may be included along the slip surfaces, which makes the overall failure probability greater
18 than any individual slip surface. In this paper, an efficient system reliability analysis concerning the
19 layered soil slopes is conducted based on the sequential compounding method (SCM) that has the
20 ability to compound multiple failure events into an equivalent event sequentially. First, the first
21 order reliability method (FORM) is employed to quantify initial reliability indices and correlation
22 coefficients among these failure modes. Subsequently, the SCM is used to calculate the equivalent
23 reliability indices and correlation coefficients until the multiple failure events are reduced to a
24 compound event, and then the system reliability of the slope is obtained accordingly. The application
25 of the approach to probabilistic evaluation of layered slopes is illustrated by two typical examples,
26 and the correctness is verified by the Monte Carlo simulation (MCS). The results show that the SCM
27 can deliver accurate system failure probability and greatly improve the computational efficiency
28 compared with the MCS, which is an advantageous and promising strategy in evaluating the system
29 reliability of layered soil slopes.

30 **Keywords:** System reliability; Layered soil slopes; Multiple failure modes; First order reliability
31 method; Sequential compounding method; Monte Carlo simulation

32

33 **Introduction**

34 There is an ever-increasing interest in evaluating the performance of the layered soil slopes
35 from the perspective of reliability analysis, because it can take into account the uncertainties that
36 exist in engineering geology widely (Cho 2009; Phoon and Ching 2015; Li and Wang 2021; Zai et

37 al. 2021; Liao et al. 2021a). Compared with conventional stability analyses assuming that the
38 geotechnical properties are constant and result in a single factor of safety, reliability analysis
39 considers the random variation of geotechnical properties and quantifies the probability of failure
40 to reflect the hazard level of slopes, which can be further applied in risk management and decision-
41 making (Zhang et al. 2013b; Hicks et al. 2014; Vardanega and Bolton 2016; Liao et al. 2021b; Jiang
42 et al. 2022). However, calculating the failure probability of individual slip surface mechanically,
43 even the most critical one, may underestimate the failure probability when the slope involves
44 multiple slip surfaces (Zhang et al. 2013a; Kang et al. 2015; Zeng et al. 2018). In this case, the
45 instability of the slope could be triggered by any mobilization of the potential slip surfaces. The
46 slope can be therefore considered as a series system.

47 In recent decades, several methods have been introduced to calculate the system reliability of
48 slopes with the rapid advance of fundamental theory and computer science. Initially, Cornell's
49 bounds method, which considers the sign of the correlation coefficient among multiple failure
50 surfaces, provides a rough range of the system failure probability (Cornell 1967). However, limited
51 by ignoring the value of the correlation coefficient, the results obtained are usually overestimated.
52 Further, Ditlevsen's bounds method solves this issue by using approximation algorithm, such as first
53 order reliability method (FORM), giving a relatively narrow probability range (Ditlevsen 1979;
54 Chowdhury and Xu 1995; Low et al. 2011; Liao et al. 2022; Low and Bathurst 2022). Although this
55 technique yields seemingly good results and is widely applied in the practical analysis, the bounds
56 can be broad when the single-mode failure probabilities are all high and the modes of failure are
57 numerous (Ang and Tang 1984). Hence, some other methods have emerged in search of more precise
58 solutions. The most representative one is the Monte Carlo simulation (MCS), which is a

59 straightforward tool to calculate system reliability and serves as an unbiased way for verifying the
60 accuracy of other methods as well (Ji and Low 2012; Jiang et al. 2015). But due to its disadvantages
61 of computational effort and time consumption, more efficient simulation methods represented by
62 importance sampling (IS), subset simulation (SS), and Latin hypercube sampling (LHS), have also
63 been implemented in this framework (Ching et al. 2009; Li et al. 2017; Guardiani et al. 2021). To
64 date, although a series of efforts have been made to calculate system reliability, it is still perplexing
65 to balance the efficiency and accuracy, especially when the system is complex.

66 Sequential compounding method (SCM) proposed by Kang and Song (2010) is developed to
67 answer the system reliability of general events through solving multivariate normal integrals, which
68 has the ability to cover the system with a variety of correlation properties even for those with
69 numerous components (Chun et al. 2015). The principle of SCM is to sequentially compound two
70 components that are coupled by a logical operation, such as union or intersection, until the
71 components of the system are reduced to a single compound event. In this way, the seemingly
72 difficulty of evaluating the comprehensive performance of a complicated event is simplified into
73 solutions of calculating equivalent reliability indices and correlation coefficients, in which the initial
74 failure probabilities of the individual events and the corresponding correlation coefficients can be
75 calculated by the FORM (Haldar and Mahadevan 2000; Cho 2013). The proposed method has
76 shown that it has major advantages in terms of computational accuracy and efficiency (Chun 2021).
77 Despite the superior properties of this method, its application in the field of geotechnical engineering,
78 including slopes, is still rarely reported except for a few studies (Johari et al. 2020; Johari and
79 Kalantari 2021).

80 The present paper intends to estimate the system reliability of layered soil slopes with multiple

81 failure modes using the SCM. The FORM is first employed to calculate the initial probability
82 information of the slope, including the failure probabilities and correlation coefficients among these
83 failure modes. Then the system reliability is evaluated by the SCM. Further, the application of the
84 approach is illustrated with two typical layered soil slopes, and the accuracy of the system failure
85 probability is verified by the MCS. It is anticipated that this study can provide a feasible strategy to
86 evaluate the comprehensive performance of the slopes even for those with a large number of slip
87 surfaces from a probabilistic point of view.

88 **Methodology**

89 **Sequential compounding method**

90 It is unpractical to determine the reliability of a complex engineering system containing
91 multiple components by direct numerical integration because of absence of closed-form solution for
92 its multi-fold integration. The SCM proposed by Kang and Song (2010) has advantages in dealing
93 with multivariate normal integrals, which is capable of yielding a satisfactory result.

94 In general, the failure of any one component will cause the system to fail as a whole for the
95 linear structure, which can therefore be regarded as a series system. Supposing a series system
96 contains n components, the two components E_1 and E_2 coupled by union can be compounded into a
97 single equivalent event E_{1or2} as:

$$98 \quad P(E_1 \cup E_2 \cup E_3 \dots \cup E_n) = P(E_{1or2} \cup E_3 \cup \dots \cup E_n) \quad (1)$$

99 where E_i , $i = 1, 2, 3, \dots, n$, denotes the event of the i th component failure, and $P(E_i)$

100 denotes the probability of the i th component failure.

101 Considering De Morgan's rule and the symmetry of the standard normal distribution, the
102 reliability index β_{1or2} of the compound event E_{1or2} can be calculated as:

$$103 \quad \beta_{1or2} = -\Phi^{-1}[P(E_1 \cup E_2)] = -\Phi^{-1}[1 - P(\bar{E}_1 \cap \bar{E}_2)] = \Phi^{-1}[P(\bar{E}_1 \cap \bar{E}_2)] \quad (2)$$

104 where Φ denotes the standard normal cumulative distribution function (CDF).

105 Let the correlation coefficient between E_1 and E_2 be $\rho_{1,2}$, which can be quantified by

106 employing the results of FORM. The FORM can not only enable the evaluation of structural
 107 performance from a probabilistic perspective, but also provide additional valuable information that
 108 can be used as the medium for further analysis, such as the design point in the standard normal space
 109 (Low et al. 2011). Hence, the $\rho_{1,2}$ can be acquired as:

$$110 \quad \rho_{1,2} = \frac{\mathbf{n}_1^{*T} \mathbf{R}^{-1} \mathbf{n}_2^*}{\beta_1 \beta_2} \quad (3)$$

111 where \mathbf{n}_1^* and \mathbf{n}_2^* denote the design points corresponding to components 1 and 2, \mathbf{R} denotes the
 112 correlation matrix of the random variables, β_1 and β_2 denotes the reliability indexes
 113 corresponding to components 1 and 2, respectively.

114 All of the terms in Eq. (3) can be given by FORM. Then Eq. (2) can be expressed as:

$$115 \quad P(\bar{E}_1 \cap \bar{E}_2) = \Phi_2(\beta_1, \beta_2; \rho_{1,2}) \quad (4)$$

116 where Φ_2 denotes the joint CDF of the bivariate standard normal distribution and can be computed
 117 by a single-fold numerical integral as:

$$118 \quad \Phi_2(\beta_1, \beta_2; \rho_{1,2}) = \Phi(\beta_1)\Phi(\beta_2) + \int_0^{\rho_{1,2}} \varphi_2(\beta_1, \beta_2; \rho) d\rho \quad (5)$$

119 where φ_2 denotes the bi-variate joint probability density function (PDF) of standard normal
 120 distribution, which can be evaluated by means of improved algorithm introduced by Genz (2004).

121 By this way, β_{1or2} can be simplified to solve:

$$122 \quad \beta_{1or2} = \Phi^{-1} \left[\Phi(\beta_1)\Phi(\beta_2) + \int_0^{\rho_{1,2}} \varphi_2(\beta_1, \beta_2; \rho) d\rho \right] \quad (6)$$

123 Once β_{1or2} is successfully calculated by the above steps, the goal turns to calculate the
 124 correlation coefficients between the equivalent event E_{1or2} and each of the other remaining
 125 components in the system.

126 Taking the three components, E_1 , E_2 , and E_i into account, the equivalent correlation coefficient
 127 can be defined as $\rho_{(1or2),i}$, which provides the same result on the probability of the event,

$$128 \quad \Omega_s = [(E_1 \leq -\beta_1) \cup (E_2 \leq -\beta_2)] \cap (E_i \leq -\beta_i), \text{ after compounding } E_1 \text{ and } E_2.$$

$$129 \quad \int_{\Omega_s} \varphi_3(E_1, E_2, E_i; \rho_{1,2}, \rho_{1,i}, \rho_{2,i}) dE = \Phi_2(-\beta_{1or2}, -\beta_i; \rho_{(1or2),i}) \quad (7)$$

130 Except for $\rho_{(1or2),i}$, all the terms in Eq. (7) are already addressed after the foregoing steps.

131 Next, decomposing the CDFs via the conditional probabilities and dividing both terms by

132 $\Phi(-\beta_i)$, the Eq. (7) is approximated as:

$$133 \quad 1 - \Phi_2(\beta_{1|i}, \beta_{2|i}; \rho_{1,2|i}) = \Phi(-\beta_{(1or2),i}) \quad (8)$$

134 The conditional reliability indices and correlation coefficients shown in Eq. (8) can be figured

135 out by the following formulas:

$$136 \quad \begin{cases} \beta_{1|i} = (\beta_1 - \rho_{1,i}A) / \sqrt{1 - \rho_{1,i}^2 B} \\ \beta_{2|i} = (\beta_2 - \rho_{2,i}A) / \sqrt{1 - \rho_{2,i}^2 B} \\ \rho_{1,2|i} = (\rho_{1,2} - \rho_{1,i}\rho_{2,i}B) / (\sqrt{1 - \rho_{1,i}^2 B} \sqrt{1 - \rho_{2,i}^2 B}) \\ \beta_{(1or2),i} = (\beta_{1or2} - \rho_{(1or2),i}A) / \sqrt{1 - \rho_{(1or2),i}^2 B} \end{cases} \quad (9)$$

137 where A and B are defined as:

$$138 \quad \begin{cases} A = \varphi(-\beta_i) / \Phi(-\beta_i) \\ B = A(-\beta_i + A) \end{cases} \quad (10)$$

139 By this way, the unknown $\rho_{(1or2),i}$ in Eq. (7) is determined avoiding possible multi-fold

140 numerical integration in conventional methods. Consequently, β_{1or2} and $\rho_{(1or2),i}$ are evaluated

141 seriatim. Even if a given system has complex logical description among the components, each

142 calculation of SCM involves only two components, so the compounding process can be

143 implemented sequentially without being affected by other logical operation.

144 **System reliability analysis for layered soil slopes**

145 Usually, a layered slope contains more than one potential slip surface. When there are several

146 potential failure modes inside the slope, the mechanical evaluation of the failure probability for each

147 mode cannot meet the actual demand, even the most dangerous one, so the goal turns to system

148 reliability analysis.

149 The factor of safety refers to the ratio of sliding resistance R to sliding force T along a given

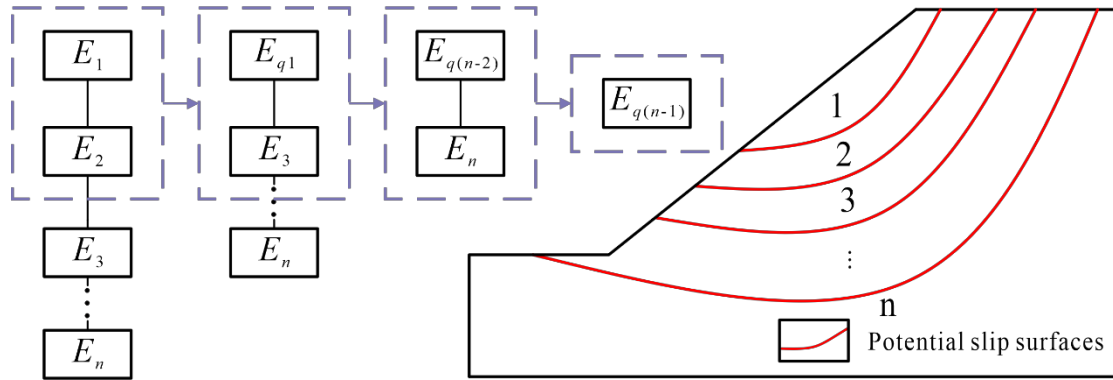
150 slip surface for the problems of slope stability, which can be denote as F_s . The limit state function

151 Z can be therefore outlined as follows:

$$152 \quad Z = g(\mathbf{X}) = R(\mathbf{X})/T(\mathbf{X}) - 1 = F_s(\mathbf{X}) - 1 \quad (11)$$

153 Considering the uncertainty of the material properties, such as strength parameters (cohesion c
 154 and internal friction angle φ), the system reliability analysis which can be also described by system
 155 failure probability P_{fs} is required for evaluating the comprehensive performance of the slope. The
 156 SCM is adopted here to achieve this goal. The implementation process of SCM with regards to a
 157 layered soil slope is shown in Fig. 1.

158



159

160 **Fig. 1.** Illustration of SCM to compute a layered soil slope.

161

162 The specific steps for implementing this approach are summarized as below, and the
 163 corresponding flowchart is shown in Fig. 2.

164 **Step 1: Set parameters.** Define the geotechnical and geometrical input parameters, including
 165 but not limited to strength parameters, unit weights, and model configuration of slope. Identify the
 166 random variables and determine its statistical characteristics, such as distribution types, means,
 167 coefficients of variation, and correlation coefficients.

168 **Step 2: Search for representative slip surfaces.** Establish the deterministic stability analysis
 169 model using the means of random variables. An in-house software and existing procedures are

170 implemented for generating the potential slip surfaces and further locating the representative slip
171 surfaces with small indices (Krahn 2004; Zhang et al. 2011).

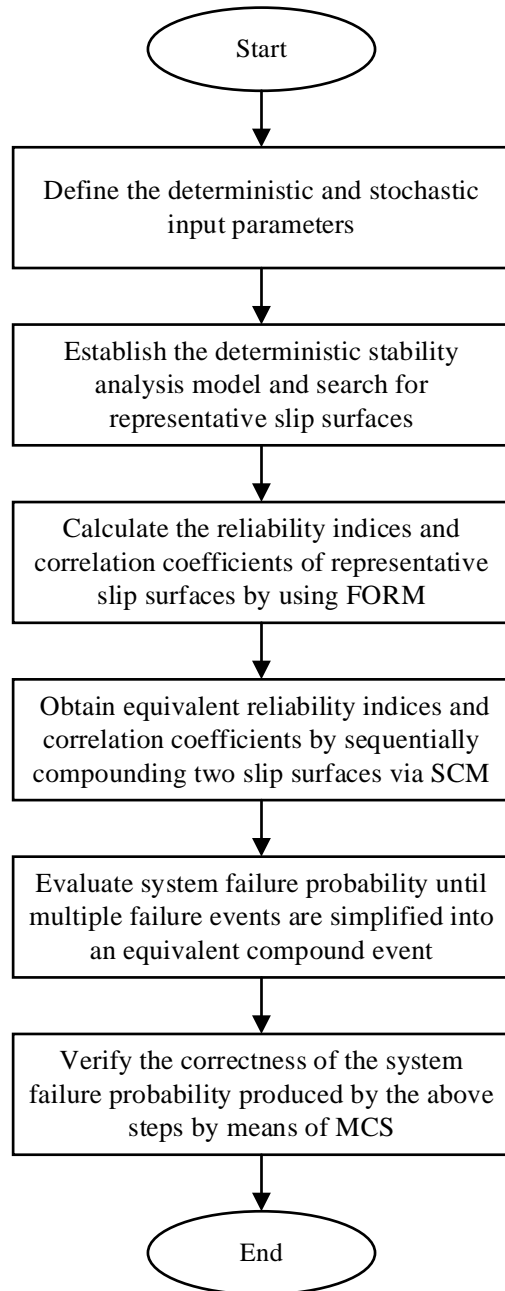
172 **Step 3:** *Calculate reliability indices and correlation coefficients.* Introduce the statistical
173 characteristics of random variables for probability analysis of the representative slip surfaces. The
174 FORM is adopted in this procedure to determine the reliability indices and correlation coefficients
175 along different representative slip surfaces, which serves as basis for subsequent analysis.

176 **Step 4:** *Obtain equivalent reliability indices and correlation coefficients.* Compound adjacent
177 reliability indices resulted in step 3 to obtain the reliability of a single equivalent failure event and
178 the correlation coefficients between this new compound event and each of the other remaining
179 failure models in the slope by using SCM.

180 **Step 5:** *Evaluate the system failure probability.* Repeat step 4 until multiple failure events are
181 simplified into an equivalent event. The system failure probability of the slope can therefore be
182 evaluated.

183 **Step 6:** *Check accuracy.* Verify the correctness of the system failure probability produced by
184 the above steps. The MCS which serves as an unbiased calculation method is conducted to achieve
185 this goal.

186



187

188 **Fig. 2.** Flowchart for evaluating the system reliability of the slope.

189

190 **Illustrative examples**

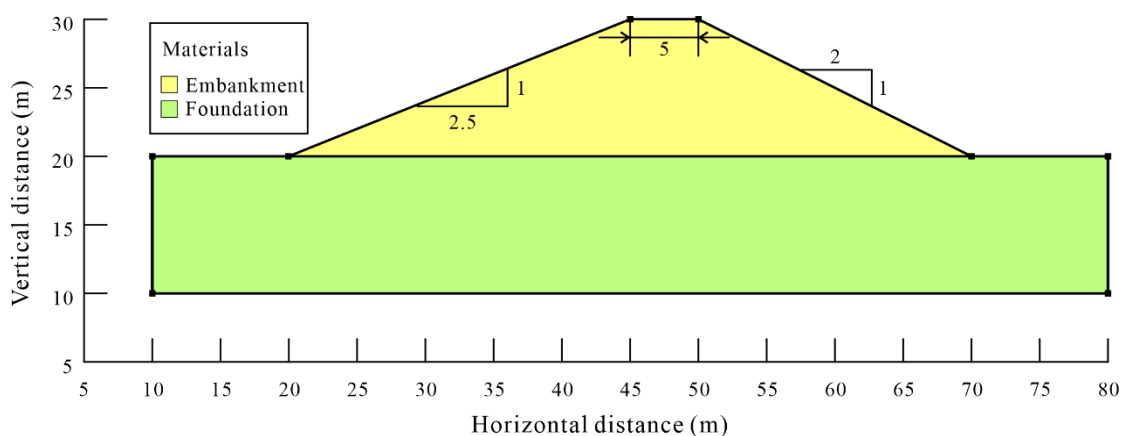
191 **Example 1: a two-layered slope**

192 The first example, a fill embankment resting on a clay layer, is adopted from Chowdhury and

193 Xu (1995). The geometry of the slope is illustrated in Fig. 3 and the material properties, including

194 deterministic and stochastic soil parameters, are given in Table 1. Among these parameters, the shear
 195 strength of the embankment and the undrained shear strength of the foundation are recognized as
 196 random variables, normally distributed and statistically independent. The unit weights of the
 197 embankment and foundation are constant.

198



199

200 **Fig. 3.** Geometry of a two-layered slope considered in example 1.

201

202 **Table 1.** Statistical properties of soil parameters in example 1

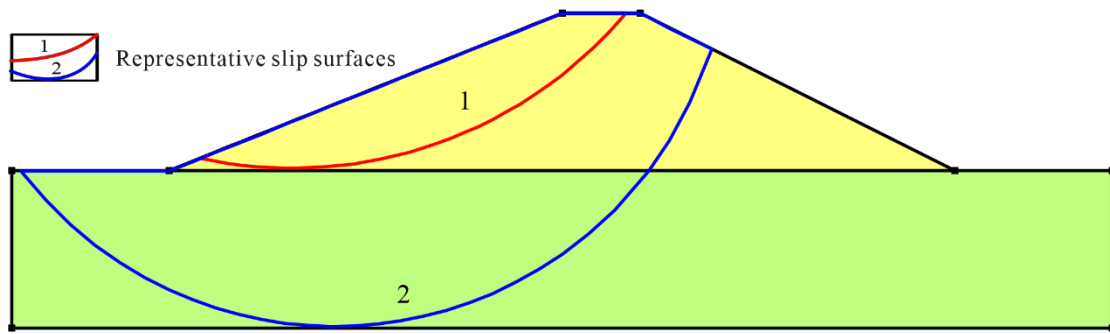
Layers	Unit weight (kN/m ³)	Cohesion (kPa)			Internal friction angle (°)		
		Mean	COV	Distribution	Mean	COV	Distribution
Embankment	20	10	0.2	Normal	12	0.25	Normal
Foundation	18	40	0.2	Normal	0	-	-

203

204 At first, the deterministic stability analysis is conducted to determine the number of potential
 205 slip surfaces using Morgenstern-Price method. The slip surfaces which are set to be circular but with
 206 different radii or centers of rotation are produced through the option of “Entry and Exit” method in
 207 Slope/W (Krahn 2004). According to Zhang et al. (2011), it is anticipated that two modes of failure

208 with the smallest β values can occur either in the embankment only or traversing both the
 209 embankment and foundation. Figure 4 shows that the two reliability-based representative slip
 210 surfaces are tangent to the bottoms of the upper and lower clay layers, respectively.

211



212

213 **Fig. 4.** Representative slip surfaces of example 1.

214

215 Once representative slip surfaces have been identified successfully, FORM can be used to
 216 estimate the failure probability of a single failure mode. Table 2 presents the FORM results,
 217 including reliability index, failure probability, design point, and correlation coefficient.

218

219 **Table 2.** FORM results of identified representative slip surfaces in example 1

Failure mode	Reliability index	Failure probability	Design point		Correlation coefficient
			x^*	x^s	
1	0.844	19.93%	-0.42	9.16	$\rho_{1,2} = 0.0582$
			-0.732	9.803	
			0	40	
2	0.819	20.65%	-0.0227	9.955	
			-0.0419	11.874	

220

221 The failure probabilities of the two circles at each design point are 19.93% and 20.65%, and
222 the correlation coefficient between the two slip surfaces is 0.0582. Further, the SCM is introduced
223 to perform system reliability analysis. Since there are only two representative slip surfaces in this
224 example, the outcome can be obtained in one step without calculating an equivalent correlation
225 coefficient. Besides, the Ditlevsen's bounds which gives the probability range of failure is calculated
226 as well, and the correctness of the system failure probability is verified by MCS with 100,000
227 samplings. Table 3 lists the results of system reliability calculation.

228

229 **Table 3.** Results of system reliability analysis for example 1.

Method	System failure probability p_{fs}
SCM	35.78%
MCS	35.92%
Ditlevsen's bounds	31.8%-36.19%

230

231 As shown in Table 3, the system failure probabilities obtained by the SCM, MCS and
232 Ditlevsen's bounds are 35.78%, 35.92%, and 31.8%-36.19%, respectively. The probability estimated
233 by the SCM is almost the same compared with MCS. On the other hand, Ditlevsen's bounds method
234 gets the system failure probability as well, but the probability range it gives is relatively extensive,
235 which cannot meet the demands of engineering practice, especially when risk control requirements
236 are stringent.

237 In addition, this typical example was also analyzed by Ji and Low (2012), Zhang et al. (2013a),
 238 and Cho (2013), and the results are listed in Table 4. Table 4 shows that the system failure probability
 239 obtained by the proposed method is close to the value that was calculated by the previous studies.

240

241 **Table 4.** Results of system reliability by different methods for example 1

Method	β_i	ρ_{ij}	P_{fs}	References
Ditlevsen's bounds	0.8471, 0.8067	0.0854	31.7-36.6%	Ji and Low (2012)
MCS with 50,000 samplings	-	-	35.75%	Ji and Low (2012)
Slide V6.0 with 2000 samplings	-	-	36.1%	Ji and Low (2012)
Ditlevsen's bounds	0.843, 0.821	0.063	31.74-36.15%	Cho (2013)
Multi-point FORM			35.94%	Cho (2013)
MCS with 20,000 samplings	-	-	36.56%	Cho (2013)
MCS with 10,000 samplings	-	-	35.6%	Zhang et al. (2013a)
SCM	0.844, 0.819	0.0582	35.78%	This study

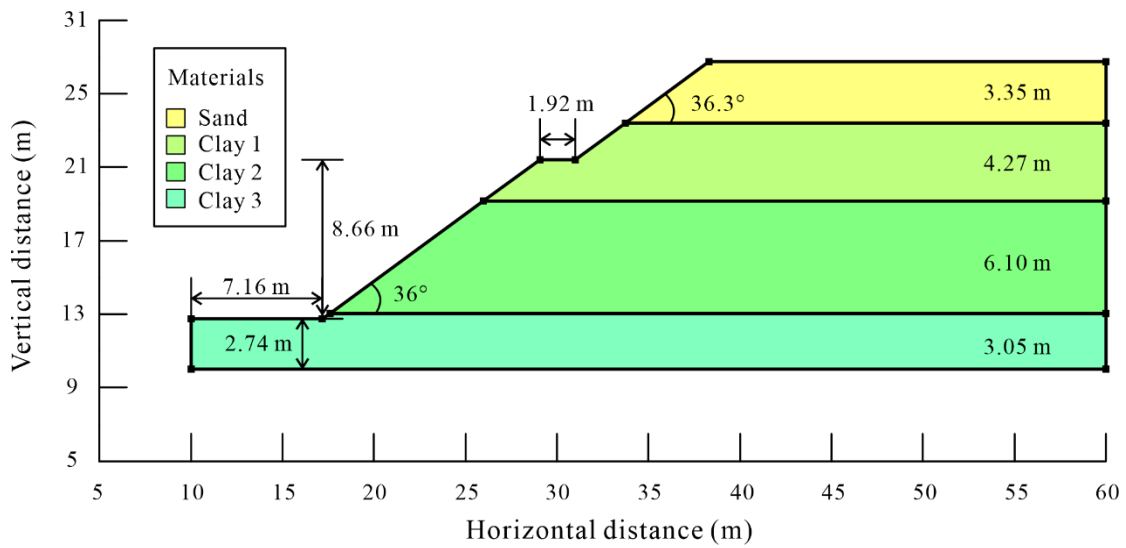
242

243 **Example 2: a multiple-layered slope**

244 The second example is a well-known real case slope with a sand fill layer overlaying three clay
 245 layers, named Congress Street Cut, and has been well documented in several publications
 246 (Chowdhury and Xu 1995; Ching et al. 2009; Ji and Low 2012; Zhang et al. 2013b; Reale et al.
 247 2016). The geometry of the slope is presented in Fig. 5. The material properties and associated
 248 uncertainties are listed in Table 5, in which the strength of the sand fill layer is defined as
 249 deterministic value while the undrained shear strengths of the three clay layers are modeled as

250 uncertain variables, normally distributed and statistically independent.

251



252

253 **Fig. 5.** Geometry of Congress Street Cut in example 2.

254

255 **Table 5.** Statistical properties of strength parameters of layers in example 2

Layers	Cohesion (kPa)			Internal friction angle (°)		
	Mean	COV	Distribution	Mean	COV	Distribution
Sand	-	-	-	30	-	-
Clay 1	55	0.37	Normal	0	-	-
Clay 2	43	0.19	Normal	0	-	-
Clay 3	56	0.24	Normal	0	-	-

256

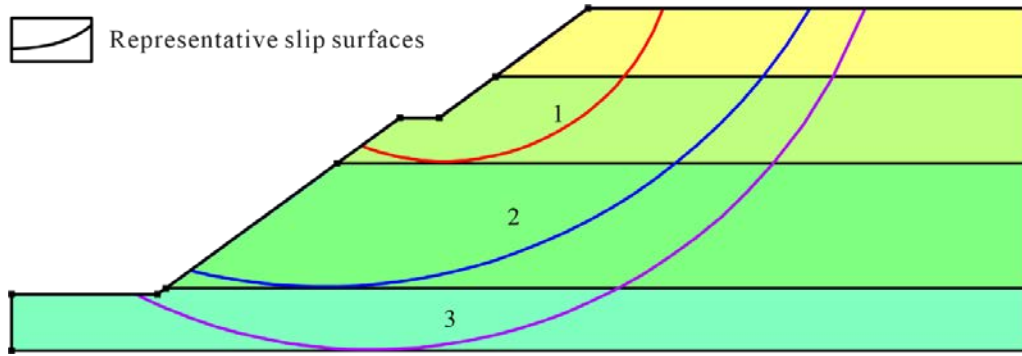
257 Likewise, three representative slip surfaces shown in Fig. 6 are located in different clay layers

258 since the circular failure can occur in any of them (Ji and Low 2012). The details of a reliability

259 assessment based on preliminary FORM are listed in Table 6.

260

261



262

263 **Fig. 6.** Representative slip surfaces of example 2.

264

265 **Table 6.** FORM results of identified representative slip surfaces in example 2

Failure mode	Reliability index	Failure probability	Design point		Correlation coefficient
			x^*	x^*	
1	1.636	5.09%	-1.636	21.709	$\rho_{1,2} = 0.398$ $\rho_{1,3} = 0.141$ $\rho_{2,3} = 0.211$
			0	43	
			0	56	
2	0.669	25.17%	-0.266	49.587	
			-0.614	37.984	
			0	56	
3	0.712	23.83%	-0.100	52.963	
			-0.121	42.015	
			-0.694	46.670	

266

267 The failure probabilities of the three slip surfaces are 5.09%, 25.17%, and 23.83%, and the
 268 correlation coefficients among the failure modes are 0.398, 0.141, and 0.211, respectively. Then the

269 SCM is employed to calculate the system failure probability, and the Ditlevsen's bounds and MCS
 270 with 100,000 samplings are adopted here as well for comparative analysis and verification.
 271 Particularly, when the Ditlevsen's bounds method is implemented, sorting the slip surfaces in
 272 descending order of probability can often produce closer bounds (Haldar and Mahadevan 2000).
 273 The results are presented in Table 7.

274

275 **Table 7.** Results of system reliability analysis for example 2

Method	System failure probability p_{fs}
SCM	42.42%
MCS	42.18%
Ditlevsen's bounds	34.86%-44.49%

276

277 As shown in Table 7, the system failure probabilities obtained by the SCM, MCS and
 278 Ditlevsen's bounds are 42.42%, 42.18%, and 34.86%-44.49%, respectively. These indicators once
 279 again prove that the proposed method can provide a satisfactory result. Furthermore, comparing the
 280 results with previous studies, Table 8 is drawn below.

281

282 **Table 8.** Results of system reliability by different methods for example 2

Method	P_{fs}	References
Ditlevsen's bounds	27.39%-44.73%	Chowdhury and Xu (1995)
MCS with 50,000 samplings	39.11%	Ji and Low (2012)
Ditlevsen's bounds	32.84%-47.57%	Reale et al. (2016)

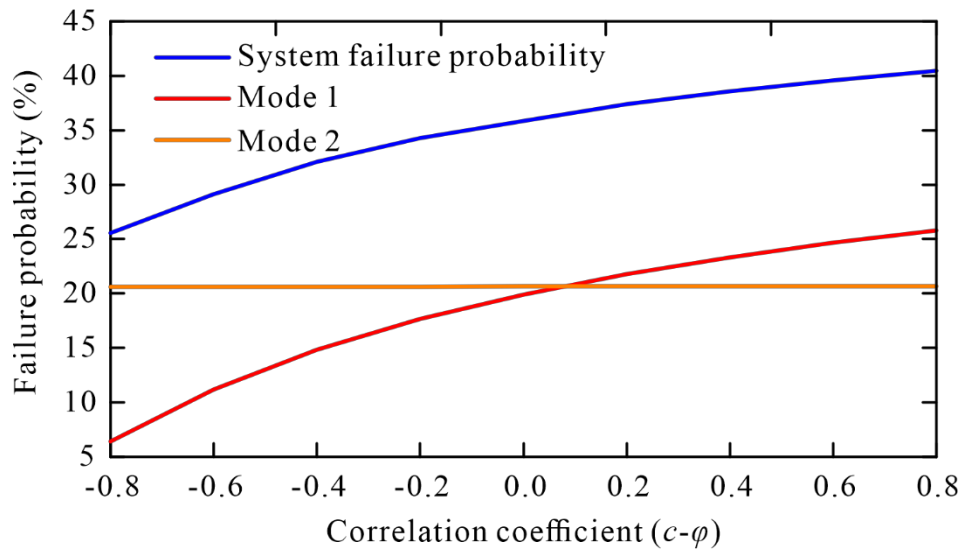
283

284 The system failure probability obtained in this study seems slightly higher, partly because all
285 three surfaces are considered here, while some studies consider only two of them (Chowdhury and
286 Xu 1995; Reale et al. 2016). Another reason behind this result is that this study specifies a denser
287 increment when defining the slip surface in Slope/W, so more failure modes are generated and the
288 representative circles with a higher probability of failure than before are located. For example, Ji
289 and Low (2012) reported that the failure probabilities of the three critical slip surfaces were 4.79%,
290 24.27% and 23.18%, but 5.09%, 25.17%, and 23.83% in this study.

291 **Discussion**

292 In the analysis of the above examples, the strength parameters of the soil layers are related to
293 c and ϕ , which are artificially assumed to be independent. In fact, the laboratory experiments have
294 suggested that the c and ϕ are often correlated, and the correlation coefficient falls between -0.72
295 and 0.35 in most tests (Lumb 1970). The method can deal not only with variables that are
296 independent but also with variables that are related. Taking the example 1 as the case study, the
297 effect of the correlation coefficient of the c and ϕ on the system reliability is illustrated supposing
298 that the correlation coefficient of embankment ranges from -0.8 and 0.8, and the results are shown
299 in Fig. 7.

300



301
302 **Fig. 7.** Results of system reliability with different correlation coefficients for example 1.

303
304 It can be seen from Fig. 7 that the probability of the mode 1 and the slope system rises as the
305 negative correlation weakens and the positive correlation increases except for mode 2 which is
306 basically unchanged during the whole range. When the correlation coefficient is -0.8, the failure
307 probabilities of mode1, mode 2, and slope system are 6.4%, 20.62%, and 25.58%; on the other hand,
308 when the correlation coefficient is 0.8, the probabilities are 25.81%, 20.68%, and 40.44%. The
309 reason behind this phenomenon is that the slip surface of mode 1 is fully located in the correlated
310 soil layer, but only a small portion of mode 2 passes through the embankment. As a result, the change
311 of correlation coefficient has a great influence on mode 1, thus improving the failure probability of
312 the system.

313 In this study, two layered soil slopes that include two and three representative slip surfaces are
314 analyzed respectively. In fact, even if the slope contains more representative slip surfaces, the SCM
315 also works (Song et al. 2021). But as the number of failure modes increases, the computation time
316 increases accordingly. In fact, in addition to the series system mentioned above, the SCM can be
317 applied to parallel, cut-set and link-set systems as well by compounding two components in

318 intersection and union flexibly (Kang and Song, 2010).

319 **Conclusions**

320 In this paper, the system reliability of layered soil slopes with multiple failure modes is
321 evaluated in the framework of SCM. In which, the FORM is employed to obtain the initial reliability
322 indices and correlation coefficients among these slip surfaces. Then the SCM is adopted to quantify
323 the system failure probability by calculating the equivalent reliability indices and correlation
324 coefficients until the slope system is simplified into a single compound event. Taking two typical
325 layered soil slopes as the case study, the SCM is implemented for the analysis of the comprehensive
326 performance of slopes, as well as the Ditlevsen's bounds method and MCS. Different from the
327 Ditlevsen's bounds method resulting in a conservative probability range, the SCM can provide an
328 exact value of the failure probability. The results from the SCM and MCS are very close, which
329 verifies the accuracy of the SCM. But compared with MCS, the SCM greatly improves the
330 calculation efficiency because it makes full use of the information resulted in FORM rather than a
331 large number of mechanical samplings as MCS, which can be a promising tool for evaluating the
332 system reliability of layered soil slopes with multiple failure modes.

333 **Data availability statement**

334 The datasets generated during and/or analyzed during the current study are available from the
335 corresponding author on reasonable request.

336 **Acknowledgements**

337 This research is supported by the National Natural Science Foundation of China (No. 41977244
338 and No. 42007267). The first author is supported by China Scholarship Council (CSC) as a visiting
339 scholar at the Leibniz University Hannover, under grant No. 202006410089. All supports are

340 gratefully acknowledged.

341 **Declaration of Competing Interest**

342 The authors declare that they have no known competing financial interests or personal
343 relationships that could have appeared to influence the work reported in this paper.

344 **References**

345 Ang, A. H. S., and W. H. Tang. 1984. *Probability Concepts in Engineering Planning and Design.*

346 *Vol. II: Design, Risk and Reliability.* New York: Wiley.

347 Ching, J., K. K. Phoon, and Y. G. Hu. 2009. "Efficient Evaluation of Reliability for Slopes with

348 Circular Slip Surfaces Using Importance Sampling." *J. Geotech. Geoenvironmental Eng.* 135

349 (6): 768–777. [https://doi.org/10.1061/\(ASCE\)GT.1943-5606.0000035](https://doi.org/10.1061/(ASCE)GT.1943-5606.0000035).

350 Cho, S. E. 2009. "Probabilistic stability analyses of slopes using the ANN-based response surface."

351 *Comput. Geotech.* 36 (5): 787–797. <https://doi.org/10.1016/j.compgeo.2009.01.003>.

352 Cho, S. E. 2013. "First-order reliability analysis of slope considering multiple failure modes." *Eng.*

353 *Geol.* 154: 98–105. <https://doi.org/10.1016/j.enggeo.2012.12.014>.

354 Chowdhury, R. N., and D. W. Xu. 1995. "Geotechnical system reliability of slopes." *Reliab. Eng.*

355 *Syst. Saf.* 47 (3): 141–151. [https://doi.org/10.1016/0951-8320\(94\)00063-T](https://doi.org/10.1016/0951-8320(94)00063-T).

356 Chun, J. 2021. "Sensitivity analysis of system reliability using the complex-step derivative

357 approximation." *Reliab. Eng. Syst. Saf.* 215: 107814.

358 <https://doi.org/10.1016/j.ress.2021.107814>.

359 Chun, J., J. Song, and G. H. Paulino. 2015. "Parameter sensitivity of system reliability using

360 sequential compounding method." *Struct. Saf.* 55: 26–36.

361 <https://doi.org/10.1016/j.strusafe.2015.02.001>.

362 Cornell, C. A. 1967. "Bounds on the reliability of structural systems." J. Struct. Div. 93 (1): 171–
363 200. <https://doi.org/10.1061/JSDEAG.0001577>.

364 Ditlevsen, O. 1979. "Narrow Reliability Bounds for Structural Systems." J. Struct. Mech. 7 (4):
365 453–472. <https://doi.org/10.1080/03601217908905329>.

366 Genz, A. 2004. "Numerical computation of rectangular bivariate and trivariate normal and t
367 probabilities." Stat. Comput. 14 (3): 251–260.
368 <https://doi.org/10.1023/B:STCO.0000035304.20635.31>.

369 Guardiani, C., E. Soranzo, and W. Wu. 2022. "Time-dependent reliability analysis of unsaturated
370 slopes under rapid drawdown with intelligent surrogate models." Acta Geotech. 17 (4): 1071–
371 1096. <https://doi.org/10.1007/s11440-021-01364-w>.

372 Haldar, A., and S. Mahadevan. 2000. *Probability, reliability, and statistical methods in engineering*
373 *design*. New York: Wiley.

374 Hicks, M. A., J. D. Nuttall, and J. Chen. 2014. "Influence of heterogeneity on 3D slope reliability
375 and failure consequence." Comput. Geotech. 61: 198–208.
376 <https://doi.org/10.1016/j.compgeo.2014.05.004>.

377 Ji, J., and B. K. Low. 2012. "Stratified Response Surfaces for System Probabilistic Evaluation of
378 Slopes." J. Geotech. Geoenvironmental Eng. 138 (11): 1398–1406.
379 [https://doi.org/10.1061/\(ASCE\)GT.1943-5606.0000711](https://doi.org/10.1061/(ASCE)GT.1943-5606.0000711).

380 Jiang, S. H., D. Q. Li, Z. J. Cao, C. B. Zhou, and K. K. Phoon. 2015. "Efficient System Reliability
381 Analysis of Slope Stability in Spatially Variable Soils Using Monte Carlo Simulation." J.
382 Geotech. Geoenvironmental Eng. 141 (2): 1–13. [https://doi.org/10.1061/\(ASCE\)GT.1943-
383 5606.0001227](https://doi.org/10.1061/(ASCE)GT.1943-5606.0001227).

384 Jiang, S. H., X. Liu, and J. Huang. 2022. “Non-intrusive reliability analysis of unsaturated
385 embankment slopes accounting for spatial variabilities of soil hydraulic and shear strength
386 parameters.” Eng. Comput. 38 (s1): 1–14. <https://doi.org/10.1007/s00366-020-01108-6>.

387 Johari, A., and A. R. Kalantari. 2021. “System reliability analysis of soldier-piled excavation in
388 unsaturated soil by combining random finite element and sequential compounding methods.”
389 Bull. Eng. Geol. Environ. 80 (3): 2485–2507. <https://doi.org/10.1007/s10064-020-02022-3>.

390 Johari, A., M. Khani, M. A. Hadianfard, and B. JavidSharifi. 2020. “System reliability analysis for
391 seismic site classification based on sequential Gaussian co-simulation: A case study in Shiraz,
392 Iran.” Soil Dyn. Earthq. Eng. 137: 106286. <https://doi.org/10.1016/j.soildyn.2020.106286>.

393 Kang, F., S. Han, R. Salgado, and J. Li. 2015. “System probabilistic stability analysis of soil slopes
394 using Gaussian process regression with Latin hypercube sampling.” Comput. Geotech. 63: 13–
395 25. <https://doi.org/10.1016/j.compgeo.2014.08.010>.

396 Kang, W. H., and J. Song. 2010. “Evaluation of multivariate normal integrals for general systems
397 by sequential compounding.” Struct. Saf. 32 (1): 35–41.
398 <https://doi.org/10.1016/j.strusafe.2009.06.001>.

399 Krahn, J. 2004. *Stability modelling with Slope/W: an engineering methodology*. Geo-Slope
400 International Ltd., Alberta, Canada.

401 Li, D. Q., Z. Y. Yang, Z. J. Cao, S. K. Au, and K. K. Phoon. 2017. “System reliability analysis of
402 slope stability using generalized Subset Simulation.” Appl. Math. Model. 46: 650–664.
403 <https://doi.org/10.1016/j.apm.2017.01.047>.

404 Li, P., and Y. Wang. 2021. “Development of an Efficient Response Surface Method for Highly
405 Nonlinear Systems from Sparse Sampling Data Using Bayesian Compressive Sensing.” J. Risk

406 Uncertainty Eng. Syst. Part A: Civ. Eng. 7 (4): 1–14. <https://doi.org/10.1061/AJRUA6.0001155>.

407 Liao, K., Y. Wu, and F. Miao. 2022. “System reliability analysis of landslides subjected to
408 fluctuation of reservoir water level: a case study in the Three Gorges Reservoir area, China.”
409 Bull. Eng. Geol. Environ. 81 (6): 1–12. <https://doi.org/10.1007/s10064-022-02698-9>.

410 Liao, K., Y. Wu, F. Miao, L. Li, and Y. Xue. 2021a. “Effect of weakening of sliding zone soils in
411 hydro-fluctuation belt on long-term reliability of reservoir landslides.” Bull. Eng. Geol.
412 Environ. 80 (5): 3801–3815. <https://doi.org/10.1007/s10064-021-02167-9>.

413 Liao, K., Y. Wu, F. Miao, L. Li, and Y. Xue. 2021b. “Time-varying reliability analysis of Majiagou
414 landslide based on weakening of hydro-fluctuation belt under wetting-drying cycles.”
415 Landslides 18 (1): 267–280. <https://doi.org/10.1007/s10346-020-01496-2>.

416 Low, B. K., and R. J. Bathurst. 2022. “Load-resistance duality and case-specific sensitivity in
417 reliability-based design.” Acta Geotech. 17 (7): 3067–3085. [https://doi.org/10.1007/s11440-](https://doi.org/10.1007/s11440-021-01394-4)
418 [021-01394-4](https://doi.org/10.1007/s11440-021-01394-4).

419 Low, B. K., J. Zhang, and W. H. Tang. 2011. “Efficient system reliability analysis illustrated for a
420 retaining wall and a soil slope.” Comput. Geotech. 38 (2): 196–204.
421 <https://doi.org/10.1016/j.compgeo.2010.11.005>.

422 Lumb, P. 1970. “Safety factors and the probability distribution of soil strength.” Can. Geotech. J. 7
423 (3): 225–242. <https://doi.org/10.1139/t70-032>.

424 Phoon, K. K., and J. Ching. 2015. *Risk and Reliability in Geotechnical Engineering*. New York:
425 CRC Press.

426 Reale, C., J. Xue, and K. Gavin. 2016. “System reliability of slopes using multimodal optimisation.”
427 Geotechnique 66 (5): 413–423. <https://doi.org/10.1680/jgeot.15.P.142>.

428 Song, J., Kang, W.-H., Lee, Y.-J., and Chun, J. 2021. "Structural system reliability: Overview of
429 theories and applications to optimization." *J. Risk Uncertainty Eng. Syst. Part A: Civ. Eng.* 7
430 (2): 03121001. <https://doi.org/10.1061/AJRUA6.0001122>.

431 Vardanega, P. J., and M. D. Bolton. 2016. "Design of Geostructural Systems." *J. Risk Uncertainty*
432 *Eng. Syst. Part A: Civ. Eng.* 2 (1): 1–12. <https://doi.org/10.1061/AJRUA6.0000849>.

433 Zai, D., R. Pang, B. Xu, Q. Fan, and M. Jing. 2021. "Slope system stability reliability analysis with
434 multi-parameters using generalized probability density evolution method." *Bull. Eng. Geol.*
435 *Environ.* 80 (11): 8419–8431. <https://doi.org/10.1007/s10064-021-02399-9>.

436 Zeng, P., T. Li, R. Jimenez, X. Feng, and Y. Chen. 2018. "Extension of quasi-Newton
437 approximation-based SORM for series system reliability analysis of geotechnical problems."
438 *Eng. Comput.* 34 (2): 215–224. <https://doi.org/10.1007/s00366-017-0536-8>.

439 Zhang, J., H. W. Huang, C. H. Juang, and D. Q. Li. 2013a. "Extension of Hassan and Wolff method
440 for system reliability analysis of soil slopes." *Eng. Geol.* 160: 81–88.
441 <https://doi.org/10.1016/j.enggeo.2013.03.029>.

442 Zhang, J., H. W. Huang, and K. K. Phoon. 2013b. "Application of the Kriging-Based Response
443 Surface Method to the System Reliability of Soil Slopes." *J. Geotech. Geoenvironmental Eng.*
444 139 (4): 651–655. [https://doi.org/10.1061/\(ASCE\)GT.1943-5606.0000801](https://doi.org/10.1061/(ASCE)GT.1943-5606.0000801).

445 Zhang, J., L. M. Zhang, and W. H. Tang. 2011. "New methods for system reliability analysis of soil
446 slopes." *Can. Geotech. J.* 48 (7): 1138–1148. <https://doi.org/10.1139/t11-009>.